Computational Materials Science 112 (2016) 467–477

Contents lists available at ScienceDirect

Computational Materials Science

journal homepage: www.elsevier.com/locate/commatsci

Theoretical studies of all-electric spintronics utilizing multiferroic and magnetoelectric materials

Wen-Yi Tong, Yue-Wen Fang, Jia Cai, Shi-Jing Gong, Chun-Gang Duan *

Key Laboratory of Polar Materials and Devices, Ministry of Education, East China Normal University, Shanghai 200062, China

ARTICLE INFO

Article history:
Received 13 April 2015
Received in revised form 4 July 2015
Accepted 7 July 2015
Available online 26 July 2015

Keywords:
Magnetoelectric effect
Multiferroic
All-electric spintronics
Rashba spin–orbit coupling
Magnetocrystalline anisotropy
Spin transport
Surface
Interface

ABSTRACT

Multiferroic and magnetoelectric materials are considered as major candidates for next-generation information storage technologies due to their simultaneous presence and interplay of two or more ferroic orders. In this paper, we briefly review our theoretical progress relating to the all-electric spintronics, i.e., spin manipulation via an electric means rather than a magnetic field. Special focus is given to interface/surface magnetoelectric effect, electric field control of magnetocrystalline anisotropy, Rashba spin–orbit coupling, spin transport, and other generalized all-electric modulation of magnetism. Our recently developed method, i.e., the orbital selective external potential method, is also expounded. This method might be a powerful tool in finding the mechanisms responsible for the intriguing phenomena occurred in multiferroics or magnetoelectric materials.

1. Introduction

Multiferroics are materials where two or more ferroic orders coexist owing to the interplay among spin, charge, lattice and orbital degrees of freedom. Coupling between electric and magnetic order parameters in multiferroic and magnetoelectric materials, i.e. magnetoelectric effect, provides an alternative way to control the magnetism electrically or dielectric properties magnetically. Many applications based on magnetoelectric effect have been proposed, including energy and frequency converter, transformer and gyrator, field sensor, modulator, signal amplifier, etc. [1]. However, the biggest impetus of the research on magnetoelectric effect probably comes from its potential application in the information processing industry. It therefore becomes the important topic of a new branch of spintronics, i.e. all-electric spintronics, which requires spin manipulation via electric means. Compared to the control of magnetization by the traditional magnetic field or the more advanced spin-current method, the electric approach has an apparent advantage, as it requires much lower power to switch the magnetization and might bring revolutions in the field of data storage with ultra-high speed and ultra-low power consumption.

In this review, we will briefly summarize our representative theoretical improvements in all-electric spintronics based on multiferroic and magnetoelectric materials. Starting from interface/-surface magnetoelectric effect, the electric field control of magnetocrystalline anisotropy, Rashba spin–orbit coupling (SOC), and spin transport will be introduced. Other generalized electrically controlled magnetism will also be discussed. Particularly, we will describe our recently developed approach, i.e. the orbital selective external potential (OSEP) method.

Due to the lack of single-phase multiferroics combining large and robust electric and magnetic polarizations at room temperature [2], the research of all-electric spintronics mainly focus on magnetoelectric compounds by artificially fabricating ferroelectrics and ferromagnets in nanoscale heterostructures. For quite a long time, the coupling between elastic components of the ferromagnetic and ferroelectric constituents through the strain is regarded as the only source of a magnetoelectric effect in composite multiferroics. As is to be shown in details later, we explored several novel magnetoelectric effects that are significantly different from traditional ones. These studies have enriched the understanding on the interactions between electric and magnetic orders in materials, and maybe helpful to the realization of magnetic manipulation via electric ways.

* Corresponding author.
E-mail address: cgduan@clpm.ecnu.edu.cn (C.-G. Duan).

http://dx.doi.org/10.1016/j.commatsci.2015.07.016
0927-0256/

2. Interface magnetoelectric effect

We first describe quantum mechanical origin of the magnetoelectric effect at the interface, which opened a new route to control magnetic properties of thin-film layered structures by electric fields. In 2006, based on first-principles calculations, Duan et al. [3] found that there exists a strong magnetoelectric effect in ferromagnetic/ferroelectric multilayers, deriving from atomic bonding at the ferromagnet/ferroelectric interface. For the Fe/$BaTiO_3$(100) heterostructure as shown in Fig. 1(a), when the $BaTiO_3$ is under the paraelectric state, the magnetic moments of the interfacial atoms are exactly the same at the bottom and top interfaces due to the structural symmetry. Note that the Fe–TiO_2 bonding results in sizeable induced magnetic moments in Ti atoms, which are antiparallel to the adjacent Fe atoms. When the inversion symmetry is broken by the upward polarized $BaTiO_3$, the Ti atoms move toward the top interface and enhances the hybridization between Fe-3*d* and Ti-3*d* orbitals at the top surface (Fig. 1(b)), which increase the induced magnetic moment on top Ti atoms but reduce the magnetic moment of top Fe atoms. Since the magnetic moments are sensitive to the interfacial bonding strength, they can be controlled by the direction of ferroelectric polarization in $BaTiO_3$. The magnetoelectric coefficient driven by interface bonding is predicted up to 0.01 G cm/V, as large as that induced by strain.

Our further study [4] revealed that the change of the interface magnetization is not the only consequence of the electric polarization reversal in such multilayers. The orbital magnetic moments and, in turn, the magnetocrystalline anisotropy energy (MAE) of Fe atoms at the interface could also be affected. As shown in Fig. 2, the magnetoelectric effect at the interface alters the MAE of a Fe monolayer by as much as 50%. With the magnetocrystalline anisotropy and the additional thickness-dependent shape anisotropy, the discovery may be helpful in writing on high coercivity perpendicular media using electric field.

Inspired by the theoretical achievements, Sahoo et al. [5] deposited a 10 nm thick Fe film on a single-crystal $BaTiO_3$(100) substrate by molecular beam epitaxy. Up to 20% coercivity change is achieved via electrical control at room temperature. Nevertheless, the polycrystalline nature of the top Fe film reveals that the primary mechanism of the magnetoelectric effect is the interface strain coupling.

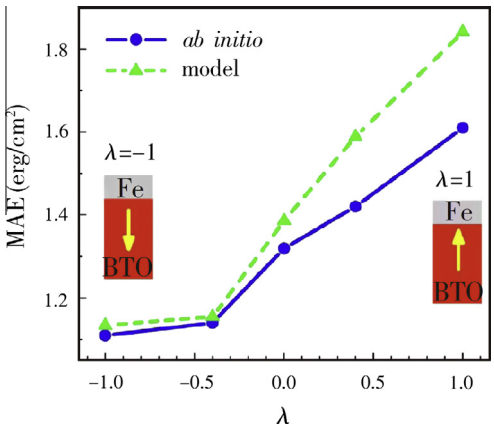

Fig. 2. MAE as a function of a polarization scaling factor λ. Here, $\lambda = 1$ and $\lambda = -1$ correspond to the spontaneous ferroelectric polarization up and down, respectively. (From Ref. [4].)

Compared with the strain-mediated magnetoelectric effect that is sensitive to the intensity instead of the direction of ferroelectric polarization, the effect driven by the ferromagnetic/ferroelectric interface bonding has the potential application in magnetic data storage without external magnetic field. In 2010, Garcia et al. [6] fabricated Fe/$BaTiO_3$/$La_{0.67}Sr_{0.33}MnO_3$ multiferroic tunnel junction and experimentally confirmed the existence of the new magnetoelectric effect. Besides the ferromagnetic/ferroelectric multilayers, the interface magnetoelectric effect has also been found in the ferrimagnetic/ferroelectric Fe_3O_4/$BaTiO_3$(001) interfaces [7].

3. Surface magnetoelectric effect

Besides the interface magnetoelectric effect in heterostructures, exploring the direct influence of an external electric field on magnetic properties of ferromagnetic metals is another important task in the research of the magnetoelectric effect.

For a ferromagnetic metal, due to the spin-dependent screening effect [8], i.e. the spin up and down electrons will have quite different responses to electric field penetrating into the ferromagnet. The spin accumulation of screening charges at the surface directly affect the surface magnetization. Since this type of magnetoelectric

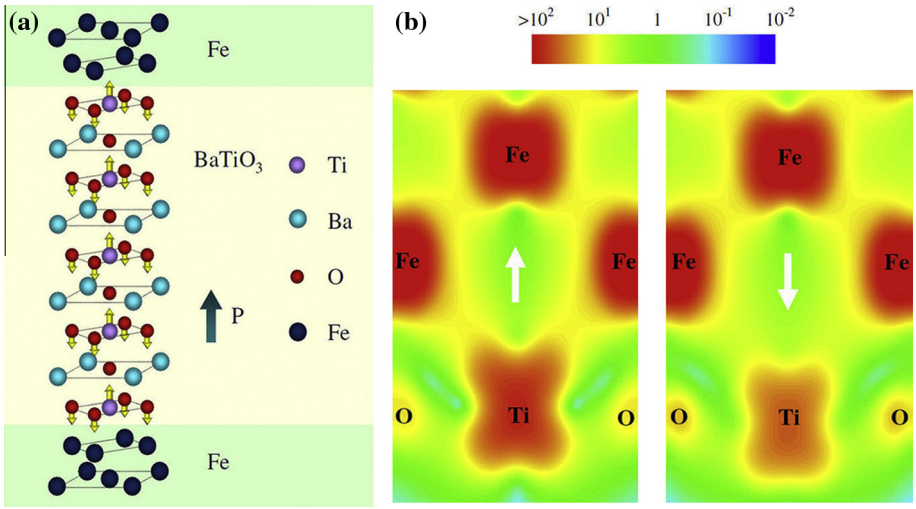

Fig. 1. (a) Atomic structure of Fe/$BaTiO_3$ multilayer for $m = 4$. (b) Minority-spin charge density at the Fe/$BaTiO_3$ interface for two opposite polarizations in $BaTiO_3$. (From Ref. [3].)

effect is essentially limited to the metal surface, it is named the surface magnetoelectric effect (see Fig. 3). Using density-functional calculations, Duan et al. [9] revealed the existence of the new effect in ferromagnetic Fe(001), Ni(001) and Co(001) films.

The screening effect of the external electric field in ferromagnetic metals is too complex to be directly described. A simple model is set up to understand the surface magnetoelectric effect. By assuming the localization of the screening charge on the metal surface and a rigid shift of the chemical potential on the surface in response to the applied electric field, the surface magnetoelectric coefficient can be obtained as [11]:

$$\alpha_s = -P_s \frac{\varepsilon \mu_B}{ec^2}, \tag{1}$$

where $P_s = \frac{n^{\uparrow}-n^{\downarrow}}{n^{\uparrow}+n^{\downarrow}}$ is the spin polarization rate of the conduction electron at the surface. ε, μ_B, e and c are dielectric constant, Bohr magneton, electron charge and speed of light, respectively. Note that dominant spin electrons at the surface are not necessarily same as that in the bulk material. The sign of the magnetoelectric coefficient reflects the relative spin orientation of the dominant conduction electron at the surface.

According to our work, besides the notable changes in the surface magnetization, the orbital moment anisotropy and the surface magnetocrystalline anisotropy are also influenced by the effect originating from spin-dependent screening of the electric field (Fig. 4), which is of considerable interest in adjusting MAE electrically.

The work mentioned above mainly focused on the surface magnetoelectric effect in the normal ferromagnetic films, in which both the majority- and minority-spin states are located near the Fermi level at the surface. However, in case of a half metal with 100% spin polarization rate, as illustrated in Fig. 5, conducting electrons are present only in one spin channel and the other is insulating. In the vacuum, the surface magnetoelectric coefficient evolves to

$$\alpha_s = \pm\frac{\mu_B}{ec^2} = \pm\frac{\hbar}{2mc^2} \approx \pm 6.44 \times 10^{-14}\,\frac{\mathrm{G\,cm^2}}{\mathrm{V}}. \tag{2}$$

The positive (negative) sign corresponds to the conducting minority- (majority-) spin states. Impressively, it suggests that the coefficient is a universal constant in a half metal and is independent to its specific components, electronic, crystal and surface structures. A theoretical research on the CrO_2 thin film done by Duan et al. [12] confirmed it.

As seen from Fig. 6, under the influence of external electric field, the consequence of spin-dependent screening is the opposite sign of the charge densities localized in the vicinity of the surfaces. The excess spin densities imply electrically induced surface magnetization. By calculating the slope of the induced magnetic moment as a function of the applied electric field, the surface magnetoelectric coefficient for the CrO_2(001) film is estimated as -6.41×10^{-14} G cm^2/V, in good agreement with the value predicted by Eq. (2). Considering that the universal surface magnetoelectric coefficient of half-metals is distinguishable from that of ordinary ferromagnetic metals, the unique feature could be used to detect half-metallicity in ferromagnetic metals.

It is obvious that the predicted coefficient of the surface magnetoelectric effect in half metals is too small to be applied in practice. Moreover, in an ordinary ferromagnetic metal, as a fraction of the universal constant mentioned in Eq. (2), the surface magnetoelectric coefficient would be even less. It seems that the surface magnetoelectric effects are significant only when the applied electric field is very large, e.g., of a few hundred mV/Å. In order to make the surface effect useful in application, a possible way to increase it is to improve the dielectric constant ε. In 2010, by studying the influence of an external electric field on magnetic properties of the Fe/MgO(001) interface, Niranjan et al. [13] found that the magnetoelectric effect on the interface magnetization and magnetocrystalline anisotropy can be substantially enhanced if the electric field is applied across a dielectric material with a large dielectric constant, as shown in Fig. 7.

In particular, we proposed that the surface magnetoelectric coefficient is larger than that for the Fe(001) surface by a factor

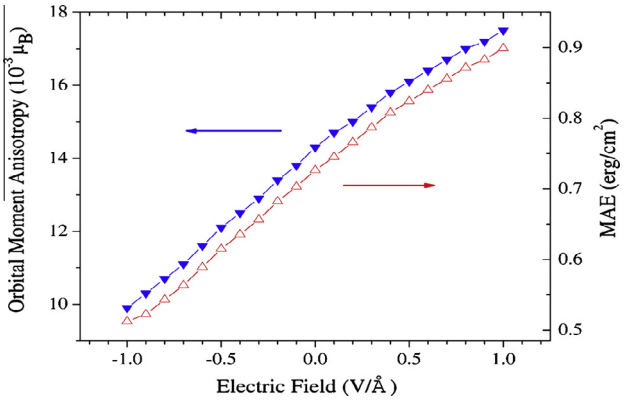

Fig. 4. Electric-field-induced changes in calculated orbital moment anisotropy (blue solid triangle line) of the surface Fe atom and surface MAE (red hollow triangle line) for 15 ML thick Fe(001) slab. (From Ref. [9].) (For interpretation of the references to colour in this figure legend, the reader is referred to the web version of this article.)

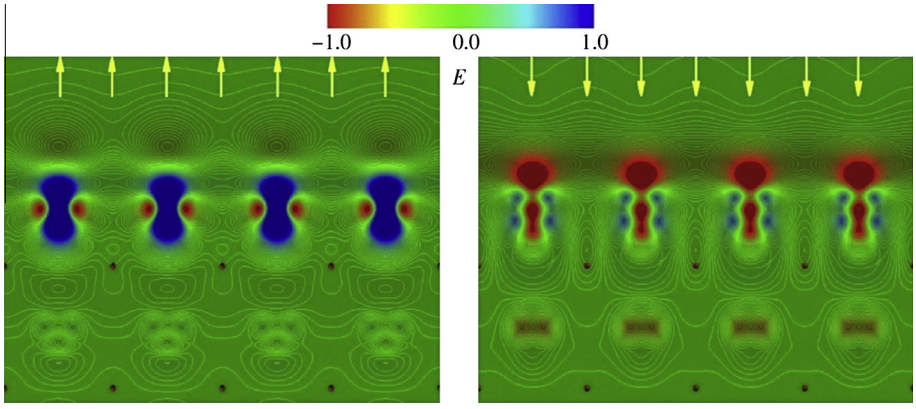

Fig. 3. Surface magnetoelectric effect of Fe film. The arrow indicates directions of the electric field. (a) Increase of the magnetization when the electric field is pointed away from the surface. (b) Decrease of the magnetization when the electric field is pointed toward the surface. (From Ref. [10].)

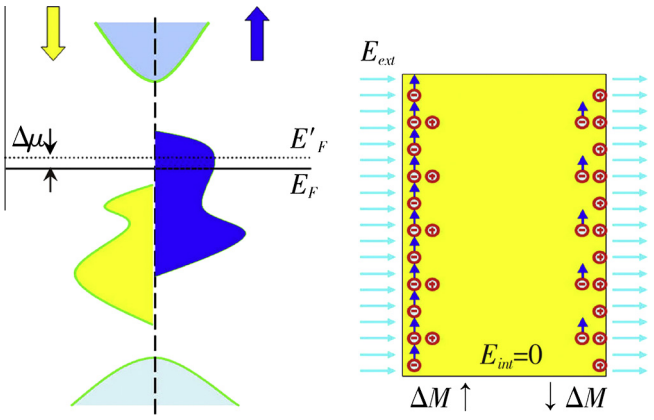

Fig. 5. Schematic of the surface magnetoelectric effect in half-metals. Due to the 100% spin polarization rate, the accumulation of charge carries at the half-metal surface induced by an electric field directly corresponds to the change of the surface magnetization. (From Ref. [10].)

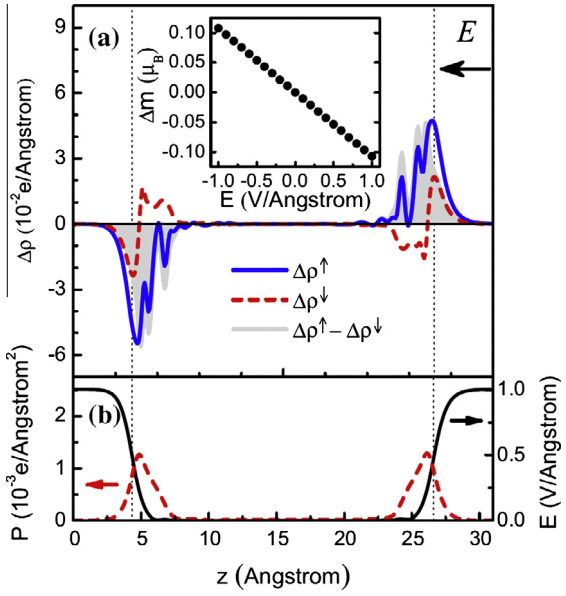

Fig. 6. Effects of electric field on electronic properties of a 22-Å-thick CrO_2(001) film along the z direction normal to the film surface. (a) Induced spin-dependent charge densities $\Delta\rho = \rho(E) - \rho(0)$ for majority-(↑) and minority-(↓) spin electrons and spin density $\Delta\rho^{\uparrow} - \Delta\rho^{\downarrow}$ averaged over the film plane. Inset: induced magnetic moment Δm per unit cell as a function of the applied electric field. (b) Variation in the electric field (solid line) and the induced minority-spin polarization (dashed line) across the film. (From Ref. [12].)

of 3.8, which is approximately equal to high frequency dielectric constant of MgO. In addition, we pointed out that the change in the relative occupancy of the 3*d*-orbitals of Fe atoms at the Fe/MgO surface significantly increases the electric field effect on the surface MAE. The enhancement of the MAE has been experimentally proved in a thin body-centered cubic Fe(001)/MgO(001) junction made by Maruyama et al. [14]. The improvement of surface magnetoelectric effects would be useful to accomplish the electrically written magnetic information technology in the future.

More comprehensive introduction of interface/surface effect is available in our reviews [10,11]. Based on the deep understanding of the relationship between magnetic and electric orders, many efforts have been made toward all-electric spintronices, including electric field control of magnetocrystalline anisotropy, Rashba SOC, spin transport and the generalized electrically controlled magnetism.

4. Electric field control of magnetic anisotropy

Directly using the surface magnetoelectric effect, Wang et al. [15] carefully designed the poly(vinylidene fluoride)(PVDF)/Fe interface structure in the PVDF/Fe/Cu/Ag heterostructure, and found that the ferroelectric polarization of PVDF can bring significant change to MAE of the Fe layer or even change the easy magnetization axis. Fig. 8 shows the designed structures. Low-density Fe monolayer causes a relatively small MAE, and the adsorption configurations of PVDF is selected to allow a strong interaction between PVDF and Fe layer. Under the circumstances, the perturbation from the ferroelectric polarization reversal can bring a substantial modification to MAE, or even alter the sign of it. The spin-dependent screening of the intrinsic electric field induced by the ferroelectric polarization of PVDF is responsible for the magnetoelectric effect. This work provides a feasible heterostructure model to realize electrical control of magnetic properties.

According to our previous work [16,17], possible effects on the magnetocrystalline anisotropy in MgO/FePt-based tunnel junctions and their origins have been systematically researched. Based on them, Zhu et al. [18] explored the dependence of MAE on the external electric field in the MgO/FePt/Pt(001) film. Using first-principles calculations, the surface magnetoelectric coefficient is estimated to be 10 times larger than that of the Fe(001) surface [9], indicating that the MAE can be linearly manipulated in a broad range by applying electric field. Considering the linear tuning effect, the Laudau–Lifshitz–Gilbert (LLG) macrospin simulation is used to investigate the coherent magnetization switching triggered by short pulses of electric-field. We found that the final state of the magnetization switching depends on the pulse time width τ. When the pulse amplitude is enhanced, the minimal critical pulse width τ_{min} decreases, whereas the maximal pulse width τ_{max} increases. In addition, by increasing the initial processional angle of the magnetization, the irregular switching would be restricted under the situation of short pulse width. A successive magnetization switching can be achieved by a series of electric field pulses, as displayed in Fig. 9.

5. Electric field control of Rashba spin splitting

SOC, which acts as a bridge between the orbital motion and spin degree of freedom, has attracted considerable research attention in the field of spintronics. Among various types of SOC, Rashba SOC [19] wins the most interest due to its tunability through an external electric field.

In order to accomplish the electric-field manipulation of the Rashba SOC, a considerable Rashba spin splitting is needed. In our previous work [20], we focused on the promising candidate material for spintronic applications – graphene. By contacting the graphene with 3*d*-ferromagnet Ni(111), we successfully enhanced its Rashba SOC, with a magnitude of up to 20 meV, which is several orders of magnitude larger than the intrinsic SOC strength in free-standing graphene. Nevertheless, it is too tiny to be used for electrically controlling spin states. Due to the much stronger Rashba spin splitting in metal surfaces, we then turned our attention to the new family for investigation of Rashba SOC.

In 2013, combining density-functional theory (DFT) calculations and theoretical analyses, Gong et al. [21] investigated the influence of the electric field on Rashba spin splitting in Au(111) surface states. We found that the applied electric field can tune the surface electrostatic potential and its gradient. Then, the change of the former induces an upward or downward shift of the surface Rashba

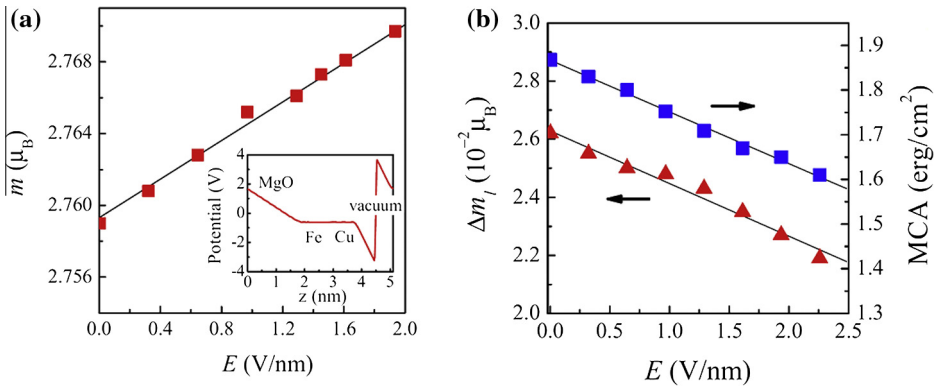

Fig. 7. (a) Magnetic moment of Fe at Fe/MgO interface as a function of the electric field in the MgO. The inset shows the calculated electrostatic potential across the supercell due to the applied electric field $E = 4$ V/nm. (b) MAE (squares) and orbital moment anisotropy (triangles) of the Fe/MgO(001) interface as a function of electric field in MgO. (From Ref. [13].)

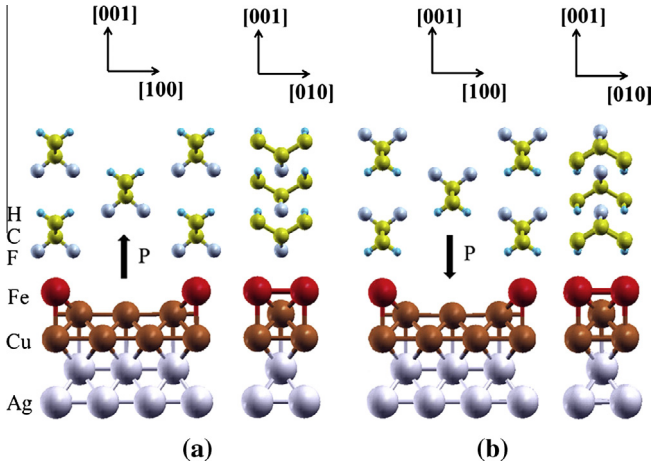

Fig. 8. Atomic structures of PVDF/Fe/Cu/Ag heterostructures with (a) Fe:F interface and (b) Fe:H interface. (From Ref. [15].)

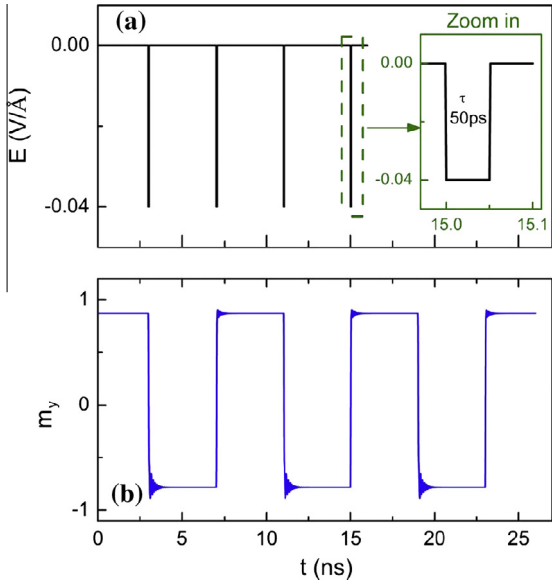

Fig. 9. The in-plane magnetization switching by multiple pulse. (a) The applied electric field pulses during the switching. (b) The magnetization switching between parallel (P) and antiparallel (AP) states. The beginning state is the P state. (From Ref. [18].)

splitting bands. While, the change of the latter increases or decreases the Rashba splitting energy, as plotted in Fig. 10. For the electric field ranging from −0.4 V/Å to 0.4 V/Å, a good linear relationship between the Rashba splitting energy and the external electric field is revealed, which is attributed to the linear response of the first-order Rashba parameter to the electric field. Nevertheless, the higher-order Rashba components are found to be less influenced by the electric field, which results in the nonlinear relationship between Rashba splitting energy and the wave vectors. The investigation about the electric field manipulation of the Rashba spin splitting in a metal surface is of great interest in the area of electrical control of spin state.

6. Electric field control of spin transport

As a well-known phenomenon in quantum mechanics, tunnel effect not only has fundamental scientific interests, i.e., it demonstrates the wave-particle dualism, but also is of great importance to modern technology. The successful application of tunnel magnetoresistance (TMR) effect [22] or giant magnetoresistance (GMR) effect [23] in hard-disk drives and magneto resistive random-access memory (MRAM) [24] drives the research of other types of tunnel effects. Considering the coexistence of electric and magnetic orders in multiferroics, which implies the feasibility of multi-state memory, multiferroic tunnel junctions (MTJs) serve as candidates in the field of all-electric spintronics (for our review see Ref. [25]).

For quite a long time, the idea to combine ferroelectricity and electron tunneling in a single device seemed to be unfeasible because quantum tunneling is only possible through barrier

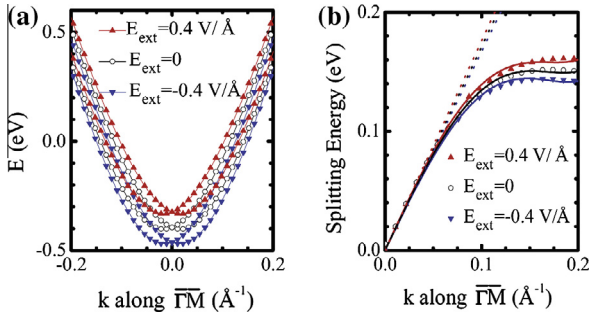

Fig. 10. (a) The surface Rashba splitting bands and (b) the Rashba splitting energies under the electric fields $\mathbf{E}_{ext} = 0$ (open circles), −0.4 V/Å (down-tirangles), and 0.4 V/Å (up-tirangles) of 22-layer Au(111) slab. (From Ref. [21].)

thickness less than a few nanometers, the scale at which ferroelectricity was thought not to exist. Until the year of 2006, Duan et al. [26] demonstrated that interfaces play an extremely critical role in the stability of nanoscale ferroelectricity. We performed a first-principles study of ultrathin $KNbO_3$ ferroelectric films placed between two metal electrodes, either $SrRuO_3$ or Pt, and proposed that nanoscale ferroelectricity is strongly affected by interfaces due to bonding of interfacial atoms in the ferroelectric to adjacent atoms in the metal electrodes. If the interface bonding is sufficiently strong, the ground state represents a ferroelectric domain with an interface domain wall [Fig. 11(a)], driven by the intrinsic oppositely oriented dipole moments at the two interfaces. The interface domain wall appears at the interface with the dipole pointed opposite to the ferroelectric polarization and plays a crucial role in the polarization pinning. An atomic-scale visualization of ferroelectric polarization pinning has been experimentally reported at coherent $BiFeO_3$(BFO)/$LaAlO_3$ interfaces in our recent work [27]. Fig. 11(b) shows that ferroelectricity can survive in a few lattice parameters. In the $KNbO_3$ films, the critical thickness is predicted to be about 1 nm for Pt and 1.8 nm for $SrRuO_3$ electrodes.

Since the ferroelectricity persists down to a nanometer scale, it is possible to use ferroelectrics as tunnel barriers in ferroelectric tunnel junctions (FTJs). Based on DFT, Velev et al. [28] studied the impact of the electric polarization on transport in Pt/$BaTiO_3$/Pt(001) tunnel junctions. It is predicted that the polarization of the $BaTiO_3$ barrier leads to a substantial drop in the tunneling conductance due to changes in the electric structure driven by ferroelectric displacements. In addition, a sizable change in the transmission probability across the Pt/$BaTiO_3$ interface with polarization reversal is found, which is generally regarded as a signature of the tunneling electroresistance (TER) effect. According to the phenomena, we reveal two important mechanisms induced by ferroelectric switching affecting the tunneling conductance in FTJs: (i) change in the electrostatic potential and the bonding at the interface, and (ii) change in the decay rates of the evanescent states in the barrier. The former alters the interface transmission function, and the latter affects the attenuation constant in the barrier. These results open interesting opportunities for improving TER effect in FTJs.

Based on the research of FTJs, we replaced the normal metal electrodes in FTJs by ferromagnetic materials, the MTJs are available. Using first principles calculation, the impact of the electric polarization on electron and spin transport was shown in Fe/$BaTiO_3$/Fe(001) MTJs [29]. We found that the influence of polarization on the tunneling conductance has different magnitudes for majority- and minority-spin channels and for parallel and antiparallel orientations of the magnetization of the electrodes. When the ferroelectric polarization of the barrier is turned on, the spin polarization of the tunneling current in the parallel configuration drops substantially. Meanwhile, an inversion of the magnetoresistance occurs. Our results indicate the possibility of electrical control of the spin polarization and TMR, as well as the exciting prospects for a four-state resistance devices using a MTJs.

In 2009, on the basis of first-principles calculations, Velev et al. [30] demonstrated four well-defined resistance states in $SrRuO_3$/$BaTiO_3$/$SrRuO_3$ MTJs. What is worth mentioning in our work is that the two asymmetrical interfaces in the tunnel junction provide the crucial structure basis for the coexistence of TER and TMR effect. As displayed in Fig. 12, due to the sensitivity of conductance to the magnetization alignment of the electrodes (TMR) and the polarization orientation in the ferroelectric barrier (TER), the resistance of such a multiferroic tunnel junction is significantly changed when the electric polarization of the barrier is reversed and/or when the magnetizations of the electrodes are switched from parallel to antiparallel. Both the calculated TMR and TER ratios are very large and dependent on the other ferroic order, revealing the strong effect of ferroelectricity on spin transport properties.

Compared to previous investigation of four-state resistive phenomenon in MTJs with multiferroic material $La_{0.1}Bi_{0.9}MnO_3$ as a barrier [31], it is advantageous to make multiferroic tunnel junctions from the combination of ferroelectric and ferromagnetic materials. The higher working temperature and relatively significant difference among conductance reveal their potential application in multilevel nonvolatile memories, tunable electric and magnetic field sensors, multifunctional resistive switches and some other multifunctional spintronic devices.

In order to improve the performance of MTJs, we made various attempts.

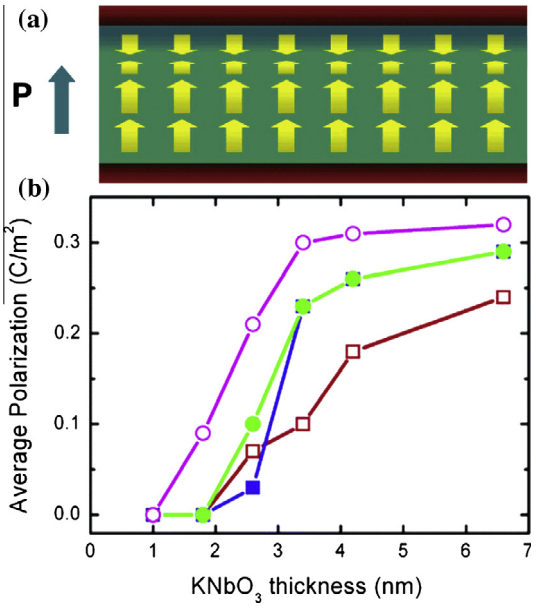

Fig. 11. (a) An interface domain-wall structure in a ferroelectric film placed between metal electrodes. The interface dipole moments are assumed to be pointed toward the ferroelectric film, and the net polarization is pointing up. (b) Average polarization as a function of $KNbO_3$ film thickness for Pt electrodes (circles) and $SrRuO_3$ electrodes (squares). (From Ref. [26].)

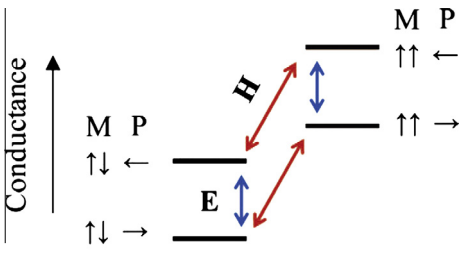

G (10^{-7} e^2/h)	↑↑	↑↓	↑↑:↑↓	TMR (%)
→	3.76	0.83	4.6	**64**
←	11.82	1.69	7.0	**75**
← : →	3.1	2.1		
TER (%)	**52**	**35**		

Fig. 12. Conductance of the $SrRuO_3$/$BaTiO_3$/$SrRuO_3$ MTJs. The four conductance states are distinguished by polarization in the barrier pointing to the left (←) or right (→) and magnetization of the electrodes being parallel (↑↑) or antiparallel (↓↓). (From Ref. [30].)

Ding et al. [32] reported a systematical study on the structural, electronic, magnetic, and ferroelectric properties of [111]-oriented BFO/$BiAlO_3$(BAO) superlattice using density-functional calculations. The inserted BAO layers greatly suppressed the Fe–O–Fe superexchange interactions. As a result, the antiferromagnetic–ferromagnetic transition energy decreased from around 280 meV per BFO formula unit to 11.6 meV per BFO/BAO formula unit. The tensile strain can further decrease the energy, making the magnetic transition more plausible. Although the magnetic properties of BFO has been greatly changed, ferroelectric polarization and energy gap of BFO are well preserved in BFO/BAO superlattice. It is obvious that constructing the BFO-based superlattice may be a good approach to improve the multiferroic behavior. Inspired by it, a multiferroic-based superlattice may be used in MTJs as a barrier.

As a practical candidate for ferromagnetic electrode material in MTJs, it is interesting to study the tetragonal $SrRuO_3$. He et al. [33] investigated its magnetic as well as the dynamical properties under the influence of epitaxial strain. As shown in Fig. 13(a), three magnetic states, i.e., nonmagnetic, strong ferromagnetic and weak ferromagnetic, are found under an in-plane compressive strain of ~4% to a tensile strain larger than 3%, which are qualitatively explained by the Stoner model. More interestingly, Fig. 13(b) reveals that metallic $SrRuO_3$ may exhibit ferroelectric-like soft mode behavior under certain strains. The strain effect in tetragonal $SrRuO_3$ might be used to tune the physical properties of MTJs. We should point out that the $SrRuO_3$ under strain could also be called *ferroelectric metal*, but may have different mechanism from that of $LiOsO_3$ [34,35]. The relevant study is currently on the way.

Layer-by-layer method is a new route to bring asymmetric ferroelectricity into the MTJs. Gao et al.'s theoretical work [36] demonstrated that the ultrathin three-component ferroelectric films have intrinsic asymmetric ferroelectricity which is robust even at the nanoscale. More interestingly, the asymmetric ferroelectricity would be more obvious when the tricolor superlattice was contacted with ferromagnetic electrode materials such as $SrRuO_3$ (Fig. 14). The finding suggests a controllable and unambiguous way to improve the working performance of MTJs, i.e. the difference between conductance states distinguished by polarization in the barrier.

7. Generalized electrically controlled magnetism

In a more general sense, the electric field control of magnetism includes not only the electrically modulated magnetization, magnetocrystalline anisotropy, Rashba SOC, and spin transport mentioned above, but also exchange bias, magnetic ordering, domain, transition temperature, etc, which provide various interesting magnetoelectric effects in both magnetoelectric compounds and single-phase multiferroics.

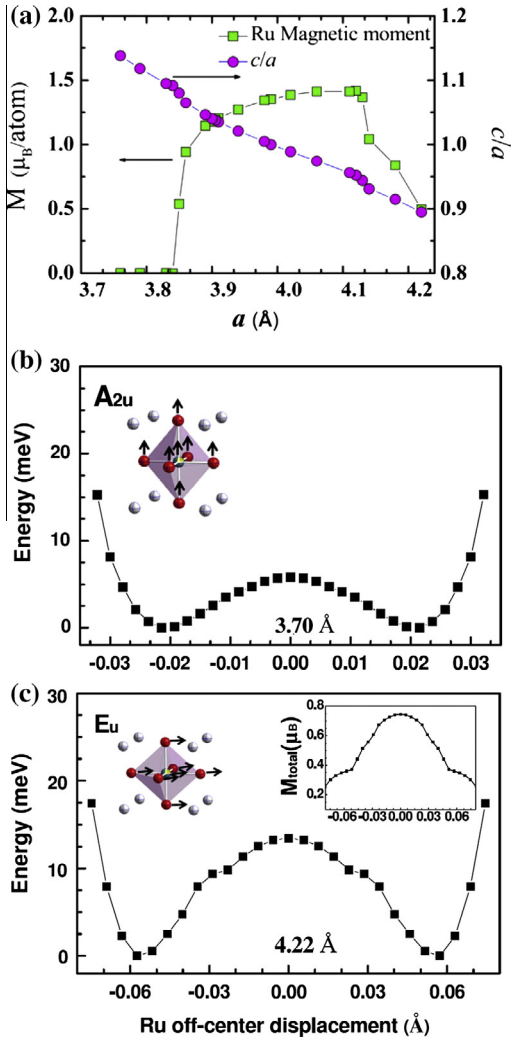

Fig. 13. (a) The magnetic moment of the Ru atom and the ratio c/a as a function of the in-plane lattice parameter. According to the unstable phonon mode of $SrRuO_3$: (b) the A_{2u} mode for compressive strain (a = 3.70 Å) and (c) the E_u mode for tensile strain (a = 4.20 Å), total energy as a function of Ru off-center displacement for lattice distortion. The inset of (c) shows the magnetic moment change with the soft mode amplitude. (From Ref. [33].)

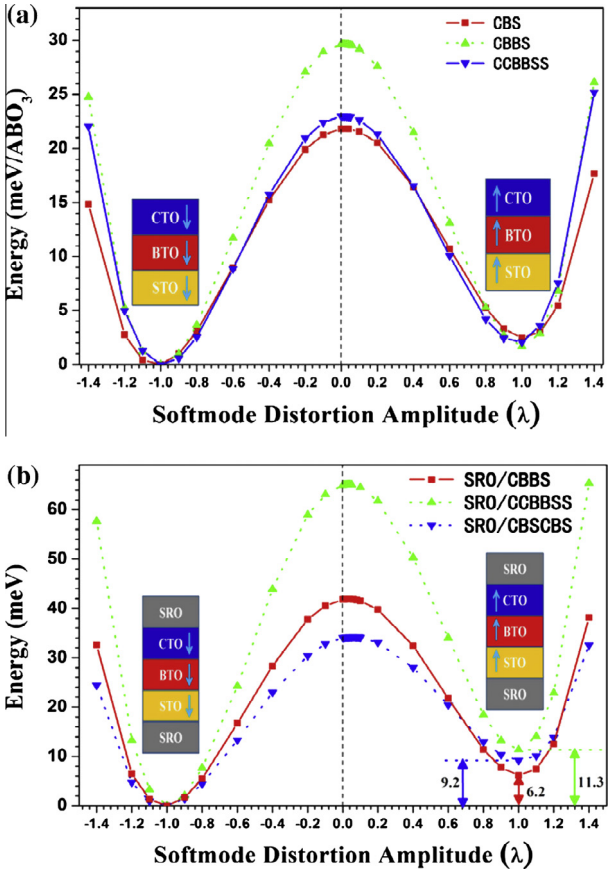

Fig. 14. Calculated asymmetric potential energy profiles of the soft mode distortions in three bulk tricolor superlattices (a) without and (b) with the electrode $SrRuO_3$. (From Ref. [36].)

Based on our early work [37–40] in the magnetic properties of the rare-earth pnictide fcc structures, we tried to control magnetic ordering by changing the Heisenberg exchange parameters through an external electric field.

As an example, Ding et al. [41] studied the relationship between the magnetic ordering and ferroelectric polarization in the tetragonal-like BFO. By using first-principles calculations, we found that there exists a transition from C1-type to G-type antiferromagnetic phase at the in-plane constant 3.91 Å when the ferroelectric polarization is along the [001] direction. The competition between the Heisenberg exchange constants J_{1c} and J_{2c} under the influence of biaxial strain is able to explain the magnetic phase transition. Interestingly, during the process of tilting the ferroelectric polarization direction by applying an external electric field, at least two effects would act on the magnetic interactions of the system. One is the strain effect reflected in the c/a ratio of the unit cell, the other is the bonding effect between Fe ions and its neighboring O atoms. Both of them could result in dramatical change of the Heisenberg exchange parameters, and then trigger the transformation of magnetic ordering. Fig. 15 displays the correlation of the magnetic ordering with lattice constant and the direction of the ferroelectric polarization. It is estimated that an electric field along the [111] direction with magnitude of 0.01 MV/cm could change the magnetic ordering from C1- to G-type antiferromagnetic ordering of tetragonal-like BFO at the lattice constant 3.87 Å.

The influence of the ferroelectric polarization on the magnetic ordering results in another, maybe more important application of multiferroic materials, i.e., spin-dependent transport. As shown in Fig. 16, different magnetic ordering causes entirely different magnetic ordering along the z direction. This will inevitably affect the spin-transport properties. By controlling the ferroelectric polarization of tetragonal-like BFO, it is possible to modulate the magnetic resistance, which provides a new avenue of information storage by electric field in a single-phase multiferroic film.

There is no doubt that the antiferromagnetic ordering can be modulated by external electric field in tetragonal-like BFO. However, the only feasible way to measure the magnetic ordering using complicated and expensive neutron scattering method greatly limit its application. Our further study explored the possibility of using a noncontact and nondestructive optical method to point out the antiferromagnetic ordering. Related work is under preparing.

Besides the external electric field, charge injection is another effective electric approach to control magnetism. Using relativistic DFT, Gong et al. [42] explored the MAE of freestanding Fe monolayer in Fe/graphene complex system. Because of the strong hybridization effect between Fe's 3d states and graphenes' p_z states, the MAE of Fe atoms is drastically suppressed from meV/atom in freestanding Fe monolayer to μeV/atom in Fe/graphene system. Even so, since the occupied Fe's 3d states introduced by the injected charge could enhance the spin and orbital magnetic moments, the suppressed MAE can be restored back by injecting charge (Fig. 17).

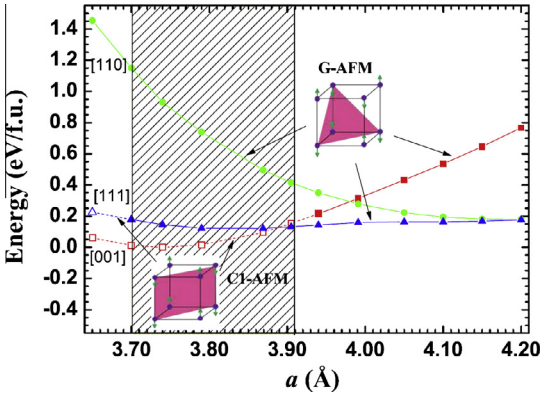

Fig. 15. Total energies with respect to the energy of [001] polarization at 3.74 Å of the tetragonal-like BFO with ferroelectric polarization along [001] (squares), [111] (triangles), and [110] (circles) directions. The straight lines with solid symbols and dotted lines with open symbols indicate the G- and C1-type antiferromagnetic ordering, respectively. The shaded zone is the possible range for the electric-field controlled C1-G phase transition. (From Ref. [41].)

Detailed progress of the physics mechanism and both theoretical and experimental improvements in the fascinating area of all-electric spintronics can be found in our recent reviews [43,44].

Apparently, the electric means has been considered as a promising and quite important way to control the magnetism. However, the practical application of it may be hindered by some shortcomings, e.g. magnetization cancelling effect, and dielectric breakdown. In order to realize the static electric field generated magnetism, more efforts should be invested in the mechanism of ferroelectricity, magnetism, and especially of magnetoelectric coupling. As an example, professor Xiangang Wan of Nanjing University and we developed a new approach, which benefits the discovery of microscopic mechanism in all-electric spintronics, and even physics research.

8. OSEP approach

In the DFT scheme of the first-principles calculations, the potential is treated as an averaged orbital-independent one-electron potential. This might be a reasonable approximation to make compromise between the complicated many-body calculations and the simple single-particle calculations when handling weakly correlated systems. However, for strongly correlated ones, ignoring the effective Coulomb repulsion (Hubbard U) results in an incorrect prediction of demanded properties, especially the energy gap. In order to overcome the deficiency, the DFT + U method was proposed to deal with many subtle problems in transition-metal oxides, rare-earth monopnictides, etc. As an example, the DFT + U method help us study the electronic structure and magnetic ordering in GdX monopnictides [38,39], as well as the optical properties in multiferroic EuO [45], whose ground state is ferromagnetic, and the ferroelectricity can be induced by epitaxial strains. Specially, the transformation first from half-metallic to semimetallic, and then ultimately to semiconducting with lattice expansion was indicated by the results of DFT + U calculations in GdN [37]. In addition, due to the DFT + U calculations of EuO, the linear and nonlinear optical response separated into different spin states directly reflect the spin-dependent band structures.

Inspired by the successful DFT + U method, we developed a new approach, i.e. OSEP method [46,47], the spirit of which is to introduce a special external potential. Different from the realistic external potential, this potential is orbital sensitive, i.e. only certain appointed orbitals can feel it. Although the orbital-sensitive potential was originally proposed for theoretical purposes, such a potential could exist in nature.

According to OSEP approach, a projector operator $|inlm\sigma\rangle\langle inlm\sigma|$ is defined, which only allows the external potential V_{ext} to influence the specific atomic orbit $|inlm\sigma\rangle$. Here i denotes the atomic site, and n, l, m, σ are the main, orbital, magnetic quantum number and spin index, respectively. Then the new Hamiltonian can be written as:

$$H^{\text{OSEP}} = H^0_{\text{KS}} + |inlm\sigma\rangle\langle inlm\sigma|V_{\text{ext}}, \tag{3}$$

where H^0_{KS} is the original Kohn–Sham Hamiltonian which includes all the orbital-independent potential. The new secular equation with this new Hamiltonian then can be solved in the framework of density functional theory in a self-consistent way, without

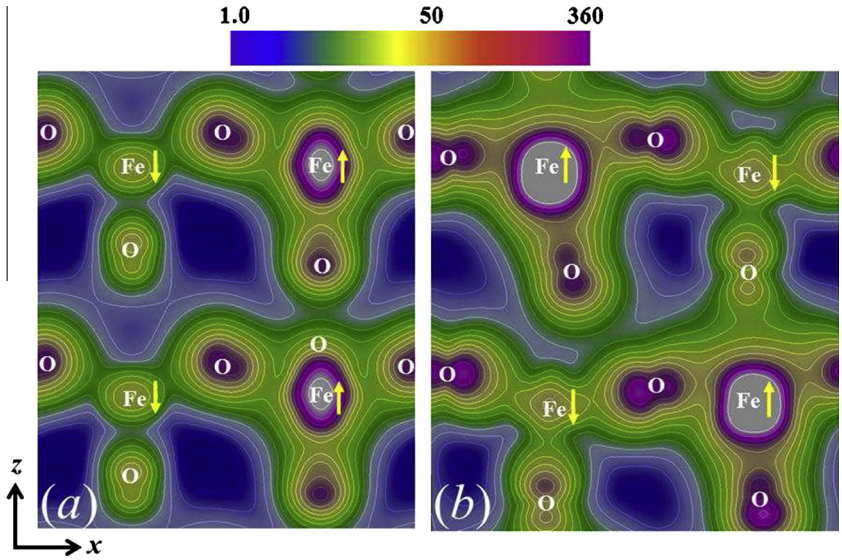

Fig. 16. Majority-spin charge density of tetragonal-like BFO at 3.79 Å when ferroelectric polarization is along (a) the [001] (C1-type antiferromagnetic ordering) and (b) the [111] direction (G-type antiferromagnetic ordering). (From Ref. [41].)

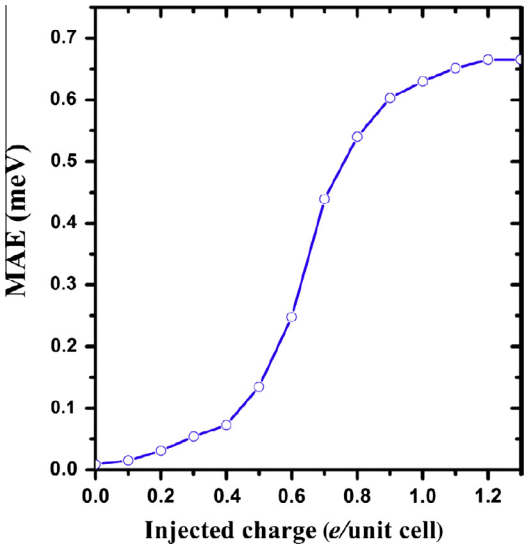

Fig. 17. Dependence of the MAE on the injected charge in Fe/graphene complex system. (From Ref. [42].)

additional efforts. In our scheme multiple orbital-dependent potentials can be applied to the system simultaneously, providing great flexibility to study various effects on the physical or chemical properties of systems. More importantly, the application of the OSEP method is not restricted in strongly correlated systems. It is of great significance in effective investigations of the origins or mechanisms of the intriguing properties of materials we are interested in.

Using such an approach, Du et al. [47] explored the mechanism of lone pairs and its stereochemical effect. The OSEP method enables us to shift the energy level of a specific atom orbital by applying an external field, and then effectively weaken or strengthen the hybridization. The lone pair should be sensitive to the shifting of the orbital if it participates in the formation of the lone pair. As shown in Fig. 18(a), an enhanced lobe-like electron density near the Pb atom is formed along the z direction of α-PbO, which is the so-called lone pair. The O 2s state is quite deep in the energy level, and therefore is negligibly responsible for the lone pair lobe. When we shift down O 2p states (Fig. 18(b)), it has almost no effect on the size and strength of lobe. However, down-shifting Pb 6s will reduce the size of the lobe (Fig. 18(c)). Moreover, up-shifting Pb 6p also weakens the lone pair, as shown in Fig. 18(d). Apparently, the on-site mixing of the cation valance s orbital with the nominally empty p orbitals of the same subshell is crucial to the formation of a lone pair. While, the anion s and p

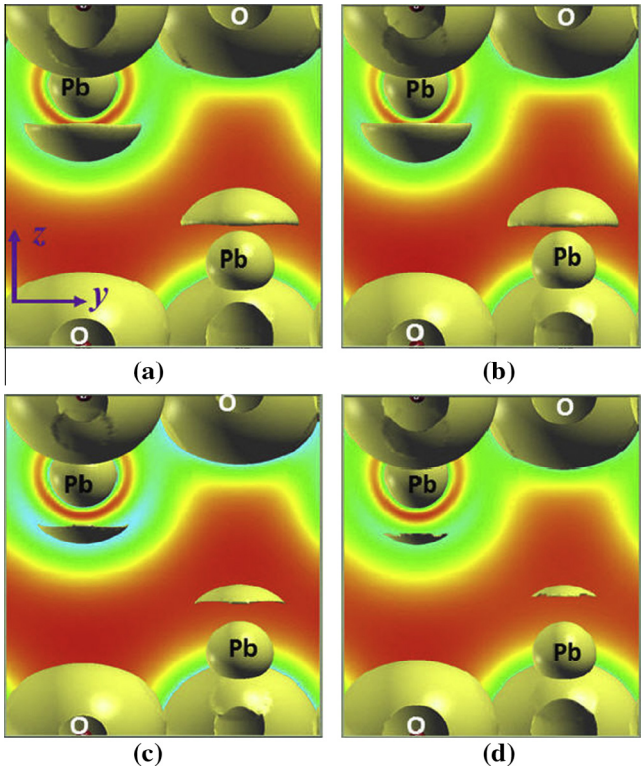

Fig. 18. Charge density contour and isosurface of α-PbO: (a) without applying a field; (b) shifting down O-2p; (c) shifting down Pb-6s; (d) shifting up Pb-6p. The lobe-like isosurface (in a golden color) near the Pb atom along the z direction indicates the appearance of a lone pair. (From Ref. [47].) (For interpretation of the references to colour in this figure legend, the reader is referred to the web version of this article.)

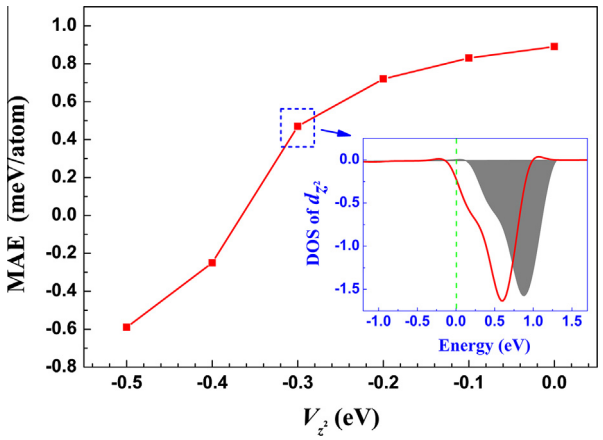

Fig. 19. MAE of monolayer Fe atoms as a function of the applied energy shift of the $3d_{z^2}$ orbital. The inset red curve shows the partial density of states (PDOS) of the minority spin channel at the $3d_{z^2}$ orbital when $V_{z^2} = -0.3$ eV. The shaded plot is the respective PDOS with $V = 0$ for comparison. Green vertical dashed line in the inset shows the Fermi level. (From Ref. [48].) (For interpretation of the references to colour in this figure legend, the reader is referred to the web version of this article.)

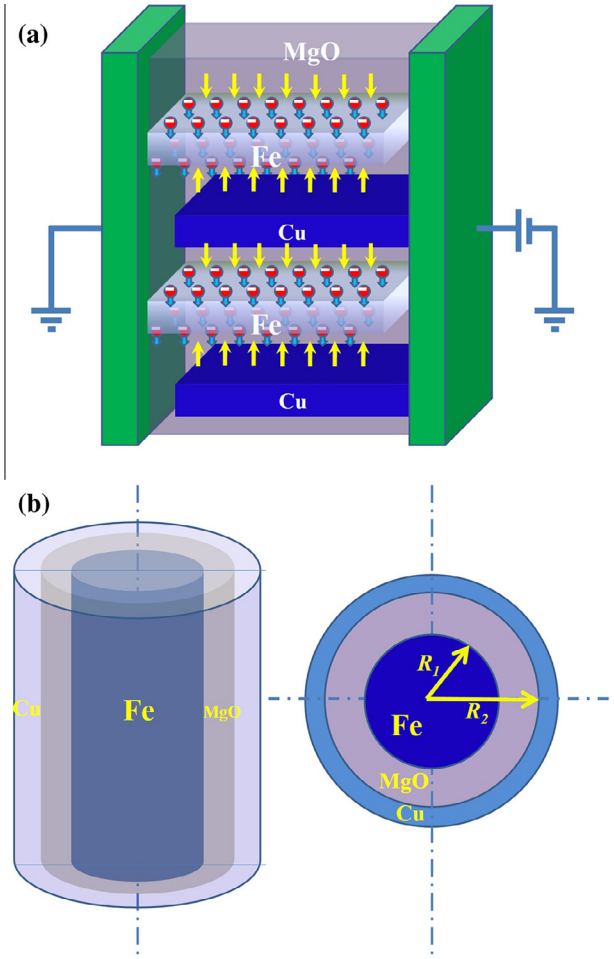

Fig. 20. Proposed new devices utilizing interface/surface magnetoelectric effect. (a) Interdigital spin capacitor; (b) coaxial cylinder spin capacitor. (From Ref. [11].)

orbitals have little effect. Our further investigation of Sn and Pb monochalcogenides shows that lone pairs are extremely sensitive to the structures of these systems. The formation of lone pairs, which can be easily controlled by our OSEP method, could, in turn, modulate the structural transition in Sn and Pb monochalcogenides.

The OSEP method is also used to identify the different contributions of each atomic orbitals to the MAE. By applying external potential on all the five 3*d* orbitals, Zhu et al. [48] proposed that the d_{z^2} electron occupation plays the most important role in the MAE of Fe monolayers and similar systems. In detail, from the inset plot of Fig. 19, we find that the applied external potential pushes the energy level of d_{z^2} downwards (compare the red solid curve and shaded plots), and results in a significant change in the occupation of d_{z^2} orbital. The occupation enhancement in the minority spin channel of the $3d_{z^2}$ orbital directly causes monotonous decrease of the MAE. Taking the Fe monolayer as a matrix, we proposed that geometrically different systems could physically modify the electron occupation of *d* orbitals, especially the $3d_{z^2}$ orbital, and then influence the magnetic properties of the magnetic film. It is possible to engineer both the MAE and the magnetic response to the electric field of the ferromagnetic metal films by adjusting the electron occupation of *d* orbitals. The OSEP method may help to open a new avenue to the artificial design of electrically controlled magnetic devices.

Based on these work, attempts have been made to uncover the microscopic formation mechanism of ferroelectricity in perovskite oxides using the OSEP method, which are of great significance in searching multiferroics with strong coupling between ferroelectricity and magnetism. Partial results is available in the chapter 3.1 in our recent review [44].

9. Discussions and conclusions

In this review, we briefly summarize representative theoretical work of our group in the booming and fascinating research branch, i.e. all-electric spintronics. Details about the progress in this and other related field based on magnetoelectirc composites [1,49–51] and single-phase multiferroics [52–54] can be found in the references. So far, various amazing achievements have been made in both the computer simulations and the experiments. Particularly, the concepts of multi-state memory [30,32,55], multiferroic random access memory [56–58], and electrically assisted magnetic recording [59] have been put forward and some of them have already been experimentally demonstrated. Nevertheless, to make multiferroic and magnetoelectric materials useful in practical application, especially in data storage technologies, it is far from enough. More efforts should be paid in the research of all-electric spintronics in both single-phase multiferroics and magnetoelectric composites.

According to the traditional point of view, magnetism and ferroelectricity tend to be mutually exclusive, as conventional ferroelectric perovskite oxides usually require transition metal ions with a formal configuration d^0, whereas magnetism, in contrast, needs partially filled *d* shells [60]. As a consequence, simultaneous multiferroics are rare. For some exceptions, e.g., BFO and $BiMnO_3$, the magnetism and ferroelectricity are widely believed to have different origins, rendering that the magnetoelectric coupling rather weak. However, our analytical and numerical analysis argued that actually simple interatomic magnetic exchange interaction already contains a driving force for ferroelectricity [61]. Searching more new microscopic mechanisms for the coexistence and strong coupling between ferroelectricity and magnetism is of both fundamental and technological interest, and might be useful to the discovery of novel multiferroics suitable for practical use with strong magnetoelectric effect and high working temperature. The OSEP approach would shed lights on our way.

For magnetoelectric multilayers, device designing is needed to maximize the interface/surface effect through enlarging the interface (surface)/bulk ratio. As an example, the interdigital spin capacitor and coaxial cylinder spin capacitor were proposed by

us [11]. In the structure shown in Fig. 20(a), the top and bottom surfaces of the same ferromagnetic metal slab, i.e. Fe, would experience the electric field of the same direction, doubling the surface magnetoelectric effect. If the non-ferromagnetic metal Cu is replaced by a ferromagnetic metal that has a different sign of the surface magnetoelectric coefficient from that of Fe, the effect will be further enhanced. In the other geometry, as proposed in Fig. 20(b), the inner Fe rod has only one surface, therefore the magnetization cancelling effect which derives from opposite electric field felt by the two surfaces/interfaces of the ferromagnetic metal could be avoided. Then, when the easy axis of the ferromagnetic rod is parallel to the axial direction, the net contribution to the magnetization due to surface magnetoelectric effect is generated.

Even if much attempts are required, we can already feel the rapid pulse of this exciting frontier. With the cooperation among theoretical research, materials designing and devices fabrication, we foresee that the application of all-electric spintronic devices in data storage with unique function and low energy consumption will be realized in the near future.

Acknowledgements

The work was supported by the National Key Project for Basic Research of China (Grant Nos. 2014CB921104 and 2013CB922301), National Natural Science Foundation of China (Grant No. 61125403), the Natural Science Foundation of Shanghai (No. 14ZR1412700), Program of Shanghai Subject Chief Scientist. Computations were performed at the ECNU computing center.

References

[1] C.-W. Nan, M.I. Bichurin, S. Dong, D. Viehland, G. Srinivasan, J. Appl. Phys. 103 (2008) 031101.
[2] N.A. Spaldin, M. Fiebig, Science 309 (2005) 391.
[3] C.-G. Duan, S.S. Jaswal, E.Y. Tsymbal, Phys. Rev. Lett. 97 (2006) 047201.
[4] C.-G. Duan, J.P. Velev, R.F. Sabirianov, W.N. Mei, S.S. Jaswal, E.Y. Tsymbal, Appl. Phys. Lett. 92 (2008) 122905.
[5] S. Sahoo, S. Polisetty, C.G. Duan, S.S. Jaswal, E.Y. Tsymbal, C. Binek, Phys. Rev. B 76 (2007) 092108.
[6] V. Garcia, M. Bibes, L. Bocher, S. Valencia, F. Kronast, A. Crassous, X. Moya, S. Enouz-Vedrenne, A. Gloter, D. Imhoff, C. Deranlot, N.D. Mathur, S. Fusil, K. Bouzehouane, A. Barthelemy, Science 327 (2010) 1106.
[7] M.K. Niranjan, J.P. Velev, C.-G. Duan, S.S. Jaswal, E.Y. Tsymbal, Phys. Rev. B 78 (2008) 104405.
[8] S. Zhang, Phys. Rev. Lett. 83 (1999) 640.
[9] C.-G. Duan, J.P. Velev, R.F. Sabirianov, Z. Zhu, J. Chu, S.S. Jaswal, E.Y. Tsymbal, Phys. Rev. Lett. 101 (2008) 137201.
[10] C.G. Duan, Prog. Phys. 29 (2009) 215 (in Chinese).
[11] C.-G. Duan, Front. Phys. 7 (2012) 375.
[12] C.-G. Duan, C.-W. Nan, S.S. Jaswal, E.Y. Tsymbal, Phys. Rev. B 79 (2009) 140403.
[13] M.K. Niranjan, C.-G. Duan, S.S. Jaswal, E.Y. Tsymbal, Appl. Phys. Lett. 96 (2010) 222504.
[14] T. Maruyama, Y. Shiota, T. Nozaki, K. Ohta, N. Toda, M. Mizuguchi, A.A. Tulapurkar, T. Shinjo, M. Shiraishi, S. Mizukami, Y. Ando, Y. Suzuki, Nat. Nanotechnol. 4 (2009) 158.
[15] R.-Q. Wang, W.-J. Zhu, H.-C. Ding, S.-J. Gong, C.-G. Duan, J. Appl. Phys. 115 (2014) 043909.
[16] W. Zhu, Y. Liu, C.-G. Duan, Appl. Phys. Lett. 99 (2011).
[17] W. Zhu, H.-C. Ding, S.-J. Gong, Y. Liu, C.-G. Duan, J. Phys.: Condens. Matter 25 (2013) 396001.
[18] W. Zhu, D. Xiao, Y. Liu, S.J. Gong, C.-G. Duan, Sci. Rep. 4 (2014) 4117.
[19] A.B. Yu, E.I. Rashba, J. Phys. C: Solid State Phys. 17 (1984) 6039.
[20] S.J. Gong, Z.Y. Li, Z.Q. Yang, C. Gong, C.G. Duan, J.H. Chu, J. Appl. Phys. 110 (2011) 043704.
[21] S.-J. Gong, C.-G. Duan, Y. Zhu, Z.-Q. Zhu, J.-H. Chu, Phys. Rev. B 87 (2013) 035403.
[22] M. Julliere, Phys. Lett. A 54 (1975) 225.
[23] M.N. Baibich, J.M. Broto, A. Fert, F.N. Van Dau, F. Petroff, P. Etienne, G. Creuzet, A. Friederich, J. Chazelas, Phys. Rev. Lett. 61 (1988) 2472.
[24] J. Åkerman, Science 308 (2005) 508.
[25] Y.-W. Fang, Y.-C. Gao, S.-J. Gong, C.-G. Duan, Prog. Phys. 33 (2013) 382 (Chinese).
[26] C.-G. Duan, R.F. Sabirianov, W.-N. Mei, S.S. Jaswal, E.Y. Tsymbal, Nano Lett. 6 (2006) 483.
[27] R. Huang, H.-C. Ding, W.-I. Liang, Y.-C. Gao, X.-D. Tang, Q. He, C.-G. Duan, Z. Zhu, J. Chu, C.A.J. Fisher, T. Hirayama, Y. Ikuhara, Y.-H. Chu, Adv. Funct. Mater. 24 (2014) 793.
[28] J.P. Velev, C.-G. Duan, K.D. Belashchenko, S.S. Jaswal, E.Y. Tsymbal, Phys. Rev. Lett. 98 (2007) 137201.
[29] J.P. Velev, C.G. Duan, K.D. Belashchenko, S.S. Jaswal, E.Y. Tsymbal, J. Appl. Phys. 103 (2008).
[30] J.P. Velev, C.-G. Duan, J.D. Burton, A. Smogunov, M.K. Niranjan, E. Tosatti, S.S. Jaswal, E.Y. Tsymbal, Nano Lett. 9 (2009) 427.
[31] M. Gajek, M. Bibes, S. Fusil, K. Bouzehouane, J. Fontcuberta, A. Barthelemy, A. Fert, Nat. Mater. 6 (2007) 296.
[32] H.-C. Ding, Y.-W. Li, W. Zhu, Y.-C. Gao, S.-J. Gong, C.-G. Duan, J. Appl. Phys. 113 (2013) 123703.
[33] H. He, H.-C. Ding, Y.-C. Gao, S.-J. Gong, X. Wan, C.-G. Duan, J. Phys.: Condens. Matter 25 (2013) 165504.
[34] Y. Shi, Y. Guo, X. Wang, A.J. Princep, D. Khalyavin, P. Manuel, Y. Michiue, A. Sato, K. Tsuda, S. Yu, M. Arai, Y. Shirako, M. Akaogi, N. Wang, K. Yamaura, A.T. Boothroyd, Nat. Mater. 12 (2013) 1024.
[35] H.M. Liu, Y.P. Du, Y.L. Xie, J.M. Liu, C.-G. Duan, X. Wan, Phys. Rev. B 91 (2015) 064104.
[36] Y.-C. Gao, C.-G. Duan, X.D. Tang, Z.G. Hu, P. Yang, Z. Zhu, J. Chu, J. Phys.: Condens. Matter 25 (2013) 165901.
[37] C.-G. Duan, R.F. Sabiryanov, J.-J. Liu, W.N. Mei, P.A. Dowben, J.R. Hardy, Phys. Rev. Lett. 94 (2005) 237201.
[38] C.-G. Duan, W.-N. Met, Physics 35 (2006) 269.
[39] C.-G. Duan, R.F. Sabiryanov, W.N. Mei, P.A. Dowben, S.S. Jaswal, E.Y. Tsymbal, Appl. Phys. Lett. 88 (2006) 182505.
[40] C.G. Duan, R.F. Sabirianov, W.N. Mei, P.A. Dowben, S.S. Jaswal, E.Y. Tsymbal, J. Phys.-Condens. Matter 19 (2007).
[41] H.-C. Ding, C.-G. Duan, Europhys. Lett. 97 (2012) 57007.
[42] S.J. Gong, C.-G. Duan, Z.-Q. Zhu, J.-H. Chu, Appl. Phys. Lett. 100 (2012) 122410.
[43] S.-J. Gong, H.-C. Ding, W.-J. Zhu, C.-G. Duan, Z. Zhu, J. Chu, Mech. Astron. 56 (2013) 232.
[44] Y.-W. Fang, H.-C. Ding, W.-Y. Tong, W.-J. Zhu, X. Shen, S.-J. Gong, X.-G. Wan, C.-G. Duan, Sci. Bull. 60 (2015) 156.
[45] W.-Y. Tong, H.-C. Ding, Y.-C. Gao, S.-J. Gong, X. Wan, C.-G. Duan, Phys. Rev. B 89 (2014) 064404.
[46] X.G. Wan, J. Zhou, J.M. Dong, Europhys. Lett. 92 (2010) 57007.
[47] Y. Du, H.-C. Ding, L. Sheng, S.Y. Savrasov, X. Wan, C.-G. Duan, J. Phys.: Condens. Matter 26 (2014) 025503.
[48] W. Zhu, H.-C. Ding, W.-Y. Tong, S.-J. Gong, X. Wan, C.-G. Duan, J. Phys.: Condens. Matter (2015).
[49] C.A.F. Vaz, J. Hoffman, C.H. Anh, R. Ramesh, Adv. Mater. 22 (2010) 2900.
[50] J. Ma, J. Hu, Z. Li, C.-W. Nan, Adv. Mater. 23 (2011) 1062.
[51] M. Bibes, J.E. Villegas, A. Barthélémy, Adv. Phys. 60 (2011) 5.
[52] C.H.I. Zhenhua, J.I.N. Changqing, Prog. Phys. 27 (2007) 225.
[53] K.F. Wang, J.M. Liu, Z.F. Ren, Adv. Phys. 58 (2009) 321.
[54] X. Huang, S. Dong, Mod. Phys. Lett. B 28 (2014).
[55] C. Israel, N.D. Mathur, J.F. Scott, Nat. Mater. 7 (2008) 93.
[56] J.F. Scott, Nat. Mater. 6 (2007) 256.
[57] M. Bibes, A. Barthelemy, Nat. Mater. 7 (2008) 425.
[58] Y.-H. Chu, L.W. Martin, M.B. Holcomb, M. Gajek, S.-J. Han, Q. He, N. Balke, C.-H. Yang, D. Lee, W. Hu, Q. Zhan, P.-L. Yang, A. Fraile-Rodriguez, A. Scholl, S.X. Wang, R. Ramesh, Nat. Mater. 7 (2008) 478.
[59] F. Zavaliche, T. Zhao, H. Zheng, F. Straub, M.P. Cruz, P.L. Yang, D. Hao, R. Ramesh, Nano Lett. 7 (2007) 1586.
[60] N.A. Hill, J. Phys. Chem. B 104 (2000) 6694.
[61] http://arxiv.org/ftp/arxiv/papers/1202/1202.3381.pdf.